JPhys Materials

PAPER • OPEN ACCESS

A strategy for 2D MXenes as thermal management materials by laser shock nanoshaping

To cite this article: Danilo de Camargo Branco and Gary J Cheng 2023 *J. Phys. Mater.* **6** 045005

View the article online for updates and enhancements.

You may also like

- Advances in theoretical calculations of MXenes as hydrogen and oxygen evolution reaction (water splitting) electrocatalysts
Pengfei Hou, Yumiao Tian, Di Jin et al.
- Synthesis and applications of MXene-based composites: a review
Umar Noor, Muhammad Furqan Mughal, Toheed Ahmed et al.
- Physical properties of 2D MXenes: from a theoretical perspective
Aurélie Champagne and Jean-Christophe Charlier

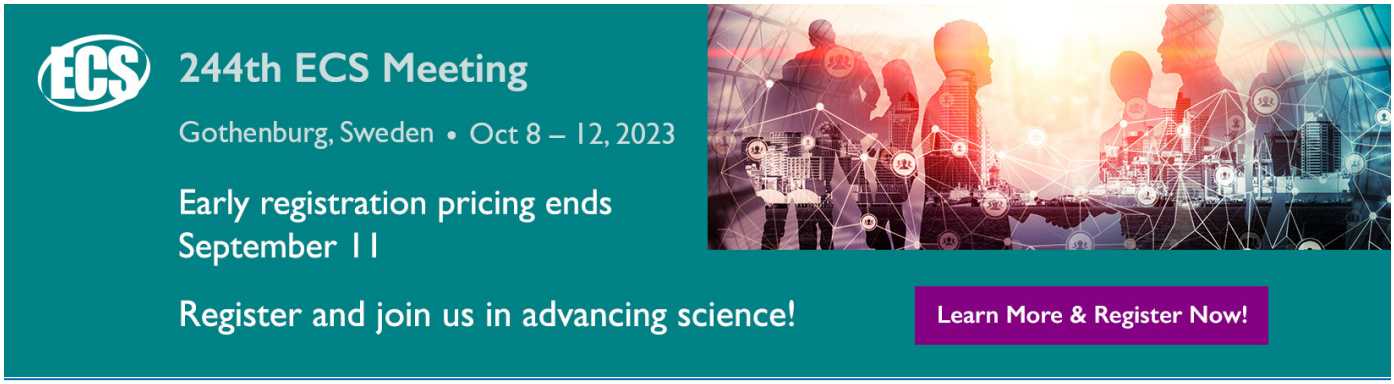

This content was downloaded from IP address 129.72.163.162 on 31/08/2023 at 01:05

Journal of Physics: Materials

PAPER

A strategy for 2D MXenes as thermal management materials by laser shock nanoshaping

Danilo de Camargo Branco[1,2] and **Gary J Cheng**[2,3,*]

[1] School of Aeronautics and Astronautics, Purdue University, West Lafayette, IN 47907, United States of America
[2] School of Industrial Engineering, Purdue University, West Lafayette, IN 47907, United States of America
[3] School of Materials Engineering, Purdue University, West Lafayette, IN 47907, United States of America
[*] Author to whom any correspondence should be addressed.

E-mail: gjcheng@purdue.edu

Keywords: 2D metamaterials, MXenes, thermal management, thermal conductivity, conformability, laser shock

Supplementary material for this article is available online

OPEN ACCESS

RECEIVED
28 March 2023

REVISED
12 July 2023

ACCEPTED FOR PUBLICATION
10 August 2023

PUBLISHED
24 August 2023

Original content from this work may be used under the terms of the Creative Commons Attribution 4.0 licence.

Any further distribution of this work must maintain attribution to the author(s) and the title of the work, journal citation and DOI.

Abstract

The two-dimensional (2D) titanium carbides ($Ti_{n+1}C_n$) belong to the MXene family, with carbon and titanium alternating in a flake structure, and are emerging options for nanoelectronics applications. In this study, the feasibility of nanoshaping of 2D titanium carbides for tunable thermal management materials was investigated. 2D titanium carbides demonstrate high degrees of formability on nanoscale and efficiency as thermal management systems in nanoelectronics components. The thermal conductivity of various MXene 2D flakes was studied using molecular dynamics simulations. A robust thermal management behavior has been predicted for 2D MXenes after nanoshaping on various nanomold patterns, which will facilitate the development of MXene-based metamaterials for thermal management in electric nanocomponents. The size dependence analysis shows that the MXenes thermal conductivity is highly influenced by the flake size leading to a variation in experimental values due to scale factors. Our model showed that Ti_2C is more sensible to strain at both supported and suspended conditions, while the thicker MXenes are not too influenced by strain. When supported, the thermal conductivities of all simulated MXenes considerably decrease due to Z phonon modes suppression. Bending strain also showed an effect in the MXenes thermal conductivity by scattering phonon modes. This makes MXenes an attractive option for the management of thermal fields.

MXenes are a two-dimensional (2D) materials family of binary, ternary, and quaternary carbides, nitrides, and carbonitrides of transition metals [1–4]. The titanium carbides with the formula ($Ti_{n+1}C_nT_x$ $n = 1$ or 2), where T_x represents the flakes' surface terminations (O, OH, or F, for example [5]), are extensively studied systems of 2D materials. These materials are promising alternatives within other 2D materials for applications such as energy storage [6], composite polymers fabrication, and thermal management within electric circuits. These titanium carbides present a 2D structure where layers of titanium are intercalated by layers of carbon atoms in a 2D hexagonal atomic structure [1] (figure 1).

Early in the MXene timeline, Kurtoglu *et al* [7], studied the elastic moduli and metallic characteristics, related to electrical conductivity, of pristine MXene sheets, without terminations, via density functional theory (DFT) calculations. Their results indicated MXenes as very stiff 2D materials (stiffness of 636 GPa for Ti_2CT_x and 523 GPa for $Ti_3C_2T_x$) when a load is applied on their basal planes. They also showed that MXenes have metallic behavior regarding electrical conductivity since the density of states at the Fermi level is high for these materials. In 2018, Borysiuk *et al* [8] executed molecular dynamics (MD) simulations to determine the bending rigidity of MXenes, proving that thicker MXenes present far better flexural rigidity than other 2D materials such as graphene and MoS_2. Lipatov *et al* [9] have performed the first nanoindentation experiments to validate simulation results and measured the $Ti_3C_2T_x$ Young's moduli (330 ± 30 GPa) and breaking strength. In 2019, Plummer *et al* [10], performed MD simulations on Ti_2CO_2 and $Ti_3C_2O_2$ to estimate Young's moduli of these materials in the presence of point defects, such as vacancies. In general,

© 2023 The Author(s). Published by IOP Publishing Ltd

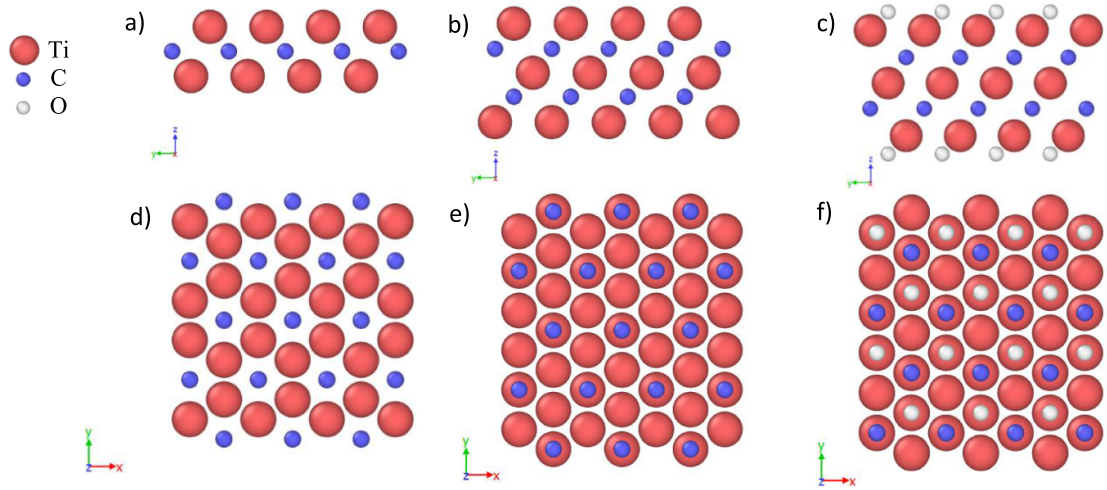

Figure 1. Side view (a)–(c) and in-plane projection (d)–(f) of three different titanium carbides (MXenes): Ti_2C, Ti_3C_2, and $Ti_3C_2O_2$ respectively.

MXenes have exhibited the highest stiffness (>330 GPa) among all solution-processed 2D materials. The current challenges for experimental validation of MXenes' physical properties lie in the fact that only small stable flakes of this 2D material can be produced, with a lateral flake size of a few tenths of μm [11, 12]. The difficulty of experimentally probing the MXene 2D flakes for their mechanical properties determination is related to the difficulty in sample preparation, and probing at such a small scale. Such difficulty is extended to probing the 2D materials' thermal properties. Therefore, experiments that use noncontact probing via laser-based technologies are employed to determine MXenes' thermal behavior [13, 14].

Thermal management using 2D materials requires knowledge of their thermal conductivities and the effects of external factors such as the substrate's material, shape, and strain induced by the substrate and deposition process. The thermal conductivity of 2D materials, when supported by a substrate, varies from its thermal conductivity when suspended within fluid media (air or liquid) [15] or in vacuum. In addition, applying strains on a 2D material may also affect its thermal conductivity [16–18]. Therefore, depending on the thermal conductivity's percentage change when supported or suspended and on the applied strain, the MXenes can be considered useful as thermal management materials. The more sensible the 2D material is to these effects, the better it is for high throughput thermal management applications. To the best of our knowledge, there have been no reports of MXene flakes thermal conductivities with flakes subjected to a high degree of conformability on textured substrates.

MXenes' thermal properties are still to be deeply explored since the research focus is currently being directed toward its energy storage, catalytic, electrical, and, more recently, mechanical properties. The in-plane MXenes thermal conductivities were evaluated by Gholivand *et al* [19]. They determined the thermal conductivity of $Ti_3C_2T_x$ via DFT and showed the effect of the termination group on the flake's thermal conductivity. The remaining challenge is the determination of in-plane thermal conductivity for the 2D $Ti_3C_2T_x$ single flakes given their size limitations, and the variety of possible terminations that can exist in a 2D flake. Motivated to fill this gap in the thermal conductivity, conformability, and strainability knowledge of the titanium carbide MXenes, we have performed a simulation-based work to verify the sensitivity of the MXene flakes' thermal conductivity to supporting conditions, strain, and conformability of these flakes. This study is necessary to verify if these 2D materials can be utilized in nanoelectronics applications for thermal management, such as thermal shifters [20] so regions within the MXene flakes can be used as thermal shields, convergers, or inverters.

Because the substrate's shape significantly alters the thermal conductivity of the 2D material [15, 20], we take advantage of this behavior to create metamaterials and tailor MXenes' thermal conductivities. In the MD simulations, we used the same principle of variations of thermal conductivities to temperature fields that were introduced by Park *et al* [20] in their temperature field manipulation using thermal shifters. Then, we used the determined thermal conductivities under the different substrate conditions to evaluate, via MD simulations, the viability of these MXenes as thermal management materials.

Another aspect of the applicability of 2D materials for thermal management is how shapeable they are and how their flakes withstand bending and in-plane strain [21]. These materials are deposited over substrates that may not be flat and must not fail when conforming to such substrates. In this study, laser

shock imprinting (LSI) was simulated to transfer the MXenes conformally on textured substrates. The bending and in-plane stresses induced by the laser shock deposition in these 2D materials, locally change their thermal conductivity due to phonons scattering at the strained regions. MD simulation results evidenced that nanoshaped $Ti_3C_2T_x$ 2D materials can be used as a thermal management metamaterial since we have verified that the MXene 2D flakes' thermal conductivity is sensitive to textured substrate conditions and can be manipulated by nanoshaping via the LSI process. The MXene flakes' manufacturing methodology impacts the type of termination (T_x) that is present in the flakes, also impacting phonon modes and consequently the flake's thermal conductivity. The flakes employed in this study had no terminations (pristine flakes) or oxygen terminations. The thermal conductivity of the flakes gets affected by the functional groups [19, 22]. Since we wanted to study the effect of the supporting and straining conditions on the flake's thermal conductivity, we focused on the oxygen terminated thermal conductivity determination via simulations for model setup, to reduce the number of force field model coefficients to be parametrized. However, the same procedure can be applied to determine the fluorine, and hydroxyl-terminated flakes' thermal conductivity for more complex force field models, considering more interatomic interactions within a MXene flake.

1. Computational methodology

The feasibility study for the 2D titanium carbides ($Ti_{n+1}C_nT_x$) as thermal management materials done in this work used computational tools for DFT calculations, equilibrium, and non-equilibrium MD (NEMD) simulations. The DFT simulations were done in *Quantum Expresso* (QE) [23]. The energy of the atomic systems for the different MXene compositions of this study (Ti_2C, Ti_3C_2, and $Ti_3C_2O_2$) were calculated in the QE tool. Some atoms in this system had their position varied and the system's energy was calculated again. With the results from the QE system energy simulations, the force field parameters for the later MD simulations were then determined by mathematically fitting the force field model that relates interatomic distances to system energy. The detailed process and the determined force field model's parameters are described and reported in the supplementary data and section 4.

After the force field model parameters were determined, equilibrium MD shock simulations were done using the LAMMPS tool [24]. This was the first modeling in this work to predict the 2D titanium carbides shapeability when shocked onto a substrate. In these simulations, the MXene flakes were accelerated and shocked over silicon substrates containing nanopillars. The MD simulations were chosen to predict if the MXene flakes would not fail when shocked onto the substrate. Silicon substrates with different nanopillar heights were used in the MD shock simulations to predict the MXene flake's behavior when the nanopillar's aspect ratio changes for a specific shock condition (represented by the flake downward acceleration setting).

The second modeling in this work considered performing NEMD simulations by setting a heat source and a heat sink to opposing sides of a rectangular MXene flake and determining the flake's thermal conductivity through the temperature field established through the flake. In this model setting, different rectangular flake sizes were simulated to determine the relationship between the flake's size and thermal conductivity. Then, we used the same type of NEMD model, but added in-plane tensile stresses by simply applying forces at one side of the rectangular flake and fixing the opposite side, and by shocking the MXene flake to a grooved substrate, causing the flake to conform to the groove and stretching it due to the flake-substrate interactions. The thermal conductivity calculation was done for the MXene flakes and the relationship between thermal conductivity and strain could be established. This type of simulation was performed for flakes without any substrate support and for flakes supported by a silicon substrate. The decision to perform supported and non-supported flakes NEMD simulations for the determination of their thermal conductivity was taken to verify the influence of supporting conditions on the flakes' thermal conductivities. The verification of the significant influence of strain and supporting conditions on the flakes' thermal conductivity helps in the conclusion of the applicability of the 2D titanium carbides as thermal management materials in nanoelectronics applications.

The third modeling in this work was like the second modeling in MD but consisted of shocking the MXene flakes against shaped substrates and simply depositing the flakes over the grooved substrates with distinct groove shapes and later performing non-equilibrium heat transfer MD simulations. These simulations were performed so the thermal shifting behavior of the simulated MXene flakes could be observed. The different substrates shapes were employed to verify how tunable the MXene flakes local thermal conductivity is by verifying strong local temperature gradient changes.

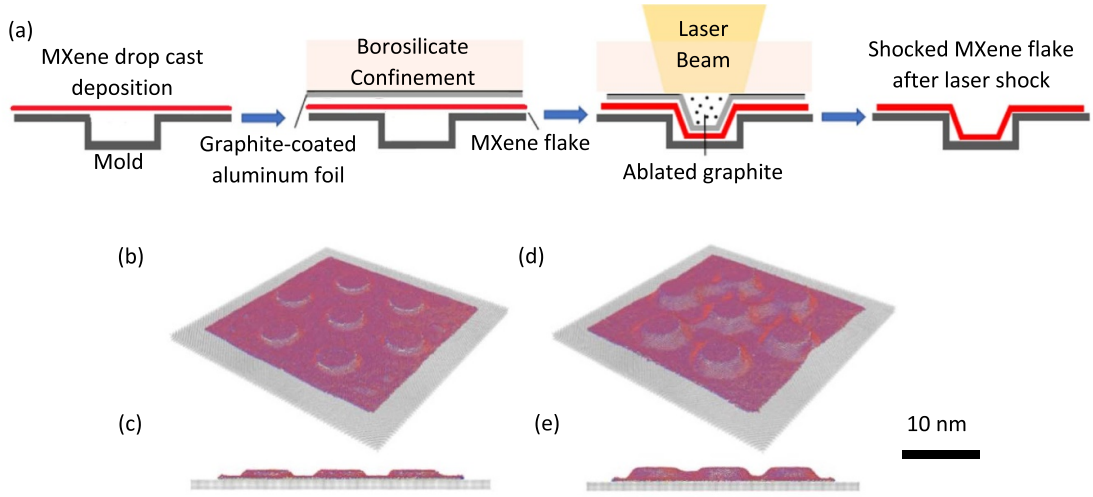

Figure 2. Conformability of MXenes on silicon substrate employing laser shocking. (a) Schematic showing the result of a drop cast MXene 2D flake deposited on a mold followed by the flake laser shocking onto the substrate improving its conformability. MD simulations showing the effects of aspect ratio (b)–(e) (pillar height/inter-pillar distance) on the formation of stress relief bumps in the flakes.

2. Results and discussions

Initially, equilibrium MD simulations where MXene flakes were accelerated above a silicon substrate with nanopillars and shocked against this substrate were executed. Figure 2(a) schematizes the LSI process through which 2D materials can be deposited over a grooved substrate. The conditions of the laser shocking process, that generate a vertical acceleration of the flake downward against the substrate, were replicated such that an equivalent flake shocking speed of approximately 800 m s^{-1} was applied to the flake, simulating the laser shocking condition from the LSI experiment [21]. In the LSI experiment, the MXene flakes that will be shocked to the substrate are first deposited via water drop casting. In this deposition process, the flakes do not wrap the substrate with good quality because of the presence of water between the flake and the substrate. After the water dries out, a borosilicate confinement with a graphene-coated aluminum foil underneath is placed over the deposited MXene flakes above the silicon substrate. When a laser pulse is focused over the experiment setup, the laser is transmitted through the borosilicate confinement, hits the graphite-coated aluminum foil, ablating the graphite, and creating a recoil pressure that builds up between the aluminum foil and the borosilicate confinement. This pressure is transmitted through the aluminum foil which accelerates the MXene flakes down, shocking the flakes against the substrate.

2.1. 2D titanium carbides shapeability

To better understand the role of the shape of the substrate on the conformal behavior of the MXene 2D flakes, we conducted MD simulations. Our MD simulation results show that, in a substrate with nanopillars, the aspect ratio between the nanopillars' height and the distance between the nanopillars dictates if small bumps in the flakes connecting the nanopillars are formed to avoid flake breakage dissipating stress. MD results show that an aspect ratio of 1.5/20 (pillar height/pillars axes distance) produces no flake bumps while an aspect ratio of 3/20 produces the bumps. Therefore, lower aspect ratios generate less stress in the 2D flakes, not requiring the flake bumps to form (figures 2(b) and (c)), while higher aspect ratios require the formation of the flake bumps to dissipate stress, avoiding flake breakage (figures 2(d) and (e)).

2.2. Size effect of 2D titanium carbides on their thermal conductivity

Continuing the feasibility study for the 2D titanium carbides as thermal management materials, it was necessary to verify the flakes' size dependence on the thermal conductivity since the current MXene flakes fabrication capabilities restrict the produced flake sizes to just a few tenths of microns. The flake size when flakes are in the submicron to low micron size scale (current MXene flake commonly achievable size), affects the flake's thermal conductivity related to lattice mobility [22]. In larger flakes, some phonon modes can be excited while such phonon modes do not have their effects accounted for in smaller flakes for the phonon's wavelength being comparable to the flake's planar dimensions. Therefore, if the currently produced flakes are employed in components fabrication, the local thermal conductivity may significantly change due to the flake size effect on thermal conductivity.

Table 1. 2D titanium carbide thermal conductivity logarithmic model parameters.

MXene type	B	M
Ti_2C	−7.91	2.54
Ti_3C_2	−8.83	2.45
$Ti_3C_2O_2$	−4.29	1.6

When the flake's temperature is altered, the lattice vibration (phonon) modes change, reaching equilibrium at different frequencies. Such phonon frequencies changes are related to anharmonic terms in the lattice potential energy, related to the lattice expansion, phonon occupation number, and anharmonic potential constants [25]. The same phonon mode changes happen when energy input is established. The energy input to the flake alters the equilibrium frequencies of the phonon modes. Each of the phonon modes is related to how well heat is transferred through the flake. For 2D materials such as MXenes, the out-of-plane (Z) phonon mode is more sensitive to temperature changes, and energy input variations, therefore having a higher influence on the 2D flake's thermal conductivity.

To understand the effect of flake size, substrate, and straining condition, on the thermal conductivity of the MXene 2D flakes, MD simulations were employed to study the local thermal behavior in MXene 2D flakes. The thermal transport NEMD flake size effect simulations show how some phonon modes do not get their effects on the thermal conductivity completely accounted for, since their wavelengths exceed the simulated flake sizes, resulting in suppression of these modes and an underestimated thermal conductivity for the MXenes (figures 3(a)–(c)). The thermal conductivity increases monotonically for Ti_2C, and Ti_3C_2 flake sizes up to a 1250 Å and for $Ti_3C_2O_2$ flake sizes up to 945 Å. Simulations with larger flakes have an impeditive computational cost considering our current computational resources. We could not check the flake size for which the thermal conductivity converges. However, we modeled the thermal conductivities (k_p) as a function of flake lateral size (L) for $Ti_3C_2O_2$, Ti_3C_2, and Ti_2C via logarithmic regressions (table 1, figures 3(a)–(c)), and equation (1). The choice of a logarithmic model for the thermal conductivity as a function of flake size is explained in the *thermal conductivity calculations* subsection of the section 4. The extrapolation of the logarithmic model for 5 μm-flake results in thermal conductivity of 19.57 W m^{-1} K for the Ti_2C, 17.68 W m^{-1} K for Ti_3C_2, and 13.02 W m^{-1} K for $Ti_3C_2O_2$. Larger extrapolations of the log models result in small thermal conductivity changes for square flakes with sides measuring above 5 μm. Zha *et al* [22] determined via DFT calculations that the thermal conductivity of M_2CO_2 (M = Ti, Zr, Hf) achieve a stable value for a flake size over 100 μm. In their research, they calculated the 5 μm flake thermal conductivity for Ti_2CO_2 in the zigzag direction as 11.91 W m^{-1} K at room temperature. The mismatch between the results obtained by Zha *et al* [22] and the results reported in this work can be explained by the influence of the oxygen termination in the MXene flake. Our simulations consider the bare flake which increased thermal conductivity in the 2D flake's zig-zag direction by 5.77 W m^{-1} K

$$k_p = B + M\ln(L) \tag{1}$$

where M and B (reported in the table 1) are the combined parameters from the phonon's thermal conductivities equations (equations (2) and (3) in the section 4), as shown in figures 3(a)–(c).

2.3. Strain effect on the flakes' thermal conductivity

After the determination of the 2D titanium carbide flake size effect on the thermal conductivity, MD non-equilibrium thermal transport simulations were done under in-plane loading conditions. This type of simulation is important in the thermal management feasibility study to verify if straining the flakes through laser shock, for example, causes a significant impact on the flake's thermal conductivity. The more significant the strain impact on thermal conductivity, the more tunable the thermal properties of the flakes are.

For all the simulated MXenes (without surface terminations and the O-terminated ones), the thermal conductivity showed a decreasing trend when the applied strains increased (figures 3(d) and (f)) for either Si-substrate supported or suspended cases. Failure of the flakes was observed at strains between 1.7% and 2.7% for $Ti_3C_2O_2$ and Ti_2C, respectively. Figures 3(e), (g) and (i) shows that the strain effect over the thermal conductivity is more pronounced for Ti_2C than Ti_3C_2 and $Ti_3C_2O_2$ for all supporting conditions. This should be happening due to the sensitivity of phonon frequencies changes to strain. For the latter flakes, the phonon frequencies and carrier velocities should not change as much as for the Ti_2C. According to Li *et al* [16], when tensile strain is applied to the basal plane of thin-film materials, their phonon diagrams have the maximum circular frequency of each phonon mode as well as acoustic phonon group velocities increased. Consequently, the phonon thermal conductivity decreases with increasing strain. Figures 3(e), (g)

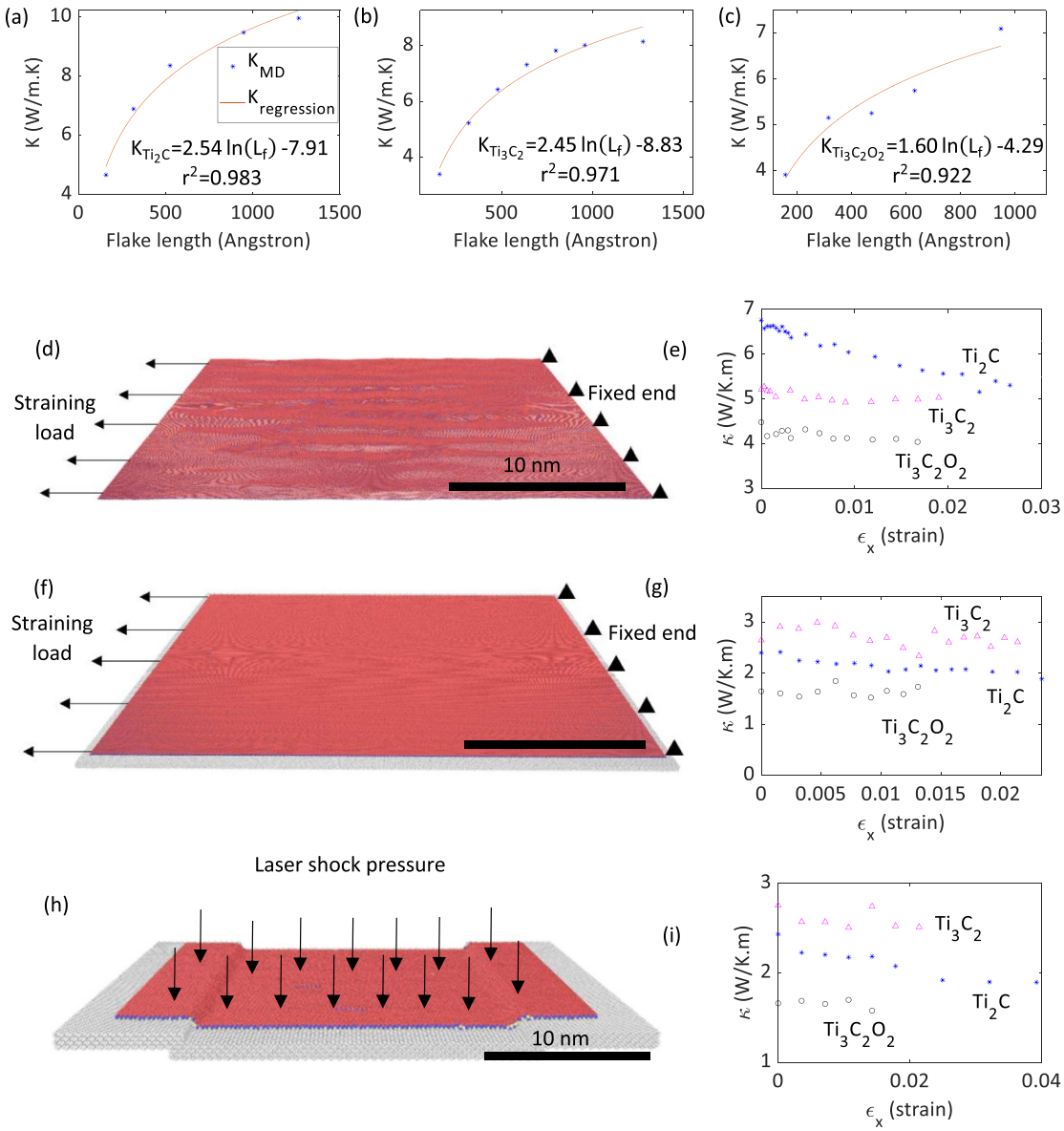

Figure 3. Thermal conductivity of MXenes. Size effect on thermal conductivity for (a) Ti_2C, (b) Ti_3C_2, and (c) $Ti_3C_2T_x$. (d), (e) Thermal conductivity dependence on strain for unsupported MXenes single flakes, and (f), (g) Si substrate supported flakes. (i) Thermal conductivity of MXene single flakes' dependence on strain induced by (h) laser shocking a single flake over a trenched Si substrate.

and (i) also shows a larger scatter in the descending thermal conductivity trends for both Ti_3C_2 and $Ti_3C_2O_2$. The two latter flakes, in the presence of defects, are still structurally sound, although these defects can considerably scatter the phonons. The Ti_2C, however, is not as susceptible to defects. Therefore, through its straining simulations, the Ti_2C flake's atomic structure is maintained without defects concentration that would significantly scatter its phonon modes.

In-plane, as well as bending strains, are developed in the MXene 2D flakes when they are shocked against grooved substrates. The results of the laser shock simulations where MXene 2D flakes were shocked onto a trenched substrate figure 3(h) show that the aspect ratio's variation directly affected the strain over the basal plane of the flakes, due to the shear forces generated by the Si substrate which prevented the flakes from relaxing and induced both bending at the trenches' edges and in plane straining. The grooves' aspect ratios are determined as the ratio between the groove's depth and width. Consequently, the 2D flakes' thermal conductivities were altered compared to the unstrained conditions. The data in figure 3(i) shows that increments of 0.0625 in the aspect ratio can impact the flake's thermal conductivity, especially for the Ti_2C. Differently from the plane strain state, the bending straining significantly scatters all phonon modes, locally decreasing the thermal conductivity. Therefore, the decrease of thermal conductivity due to the shocking of the 2D materials on a trenched substrate is attributed to the contributions of the plane strains (due to

substrate-induced friction constraining the lateral and transversal in-plane phonon modes LA, and TA, respectively) away from the trenches' edges, bending straining at the trenches' edges, and Z phonon modes restriction due to the flake–substrate interactions.

2.4. Substrate effect on the flakes' thermal conductivity

The support of a substrate to the 2D titanium carbide flakes can affect its thermal conductivity. The significance of this effect is an important aspect of the applicability of this material for thermal management similar to the effect caused by straining the flakes. The effect of the Si substrate on MXene thermal conductivity was measured through NEMD thermal transport simulations at the Ti_2C, Ti_3C_2, and $Ti_3C_2O_2$. We noticed an expressive thermal conductivity drop for the Si substrate-supported MXenes shown by the simulation results in figures 3(f) and (g), where the ZA branch suppression by the flake–substrate interaction causes a larger drop in thermal conductivity than the drop caused by in-plane straining. This drop is explained by the suppression of the Z phonon modes, which correspond to a significant fraction of the 2D materials' thermal conductivity [15]. The interactions between the silicon atoms and the MXene flakes greatly restrict the flake's lattice vibrations in the direction normal to the substrate (Z-direction or out-of-plane direction of atomic motion). We have also noticed a softer thermal conductivity decrease for supported flakes with increasing strains applied on their basal planes when compared with simulations on the suspended MXene 2D flakes. This result can be explained by the fact that in-plane phonon modes (LA and TA which are the longitudinal and transversal in-plane directions of motion for the lattice vibrations) are less affected by in-plane applied strains since the atoms' movement restrictions imposed by increased strain are less severe than the restriction imposed by the physical barrier of the substrate.

2.5. Flakes shocking over shaped substrates for thermal shifting behavior creation

The NEMD simulation results for the strained MXene flakes, which show that thermal conductivity is affected by the in-plane strain, indicated that depending on how strain is applied to the flake, the thermal conductivity may locally change. Tunning the thermal conductivity locally is a factor that is desirable in the design of a thermal metamaterial. The local tunning of the applied strain can be done by altering the substrate's shape. In practice, the production of specific and precisely shaped grooved substrates involves expensive and complex processes. One way to produce such substrates with submicron details is via laser-assisted direct nanoimprint lithography [26].

We chose multiple different substrate shapes to perform the shock MD simulations so we could see how sensitive to different local strain fields the MXene flakes' thermal conductivity is by verifying how strong the resulting thermal shifting effects are. The application of a laser shock over the MXene 2D flake (Ti_2C in the simulations reported in figure 4) changes the temperature gradients within a temperature field. In the shock deposition, the MXene 2D flake wraps the grooved substrate. This causes localized bending (figure 4(a)), and flake–substrate friction that induce bending and in-plane strains which scatter the phonon modes reducing the thermal conductivity of the flake close to the bending region. This thermal conductivity sudden reduction at the bending stress zone causes a localized steep temperature gradient.

The volumetric atomic strain (calculated via equations (6) and (7) in the section 4) at the top Ti atoms, away from the Si substrate, is in a tensile state at the top of the trench edge, and compressive strain at its bottom. The bottom Ti atoms are in a compressive state at the top of the trench edge, and tensile strain at its bottom. The middle C atoms are homogeneously at a low tensile strain due to the overall flake stretching enabled by the flake/substrate interactions (figures 4(n)–(s)). Through the flake, a few atoms have their volumetric strain significantly deviating from the flake's average strain. Those sites are defects caused by the strong loads from the shock interaction between the MXene 2D flake and the Si substrate.

At the bending locations, there is a dwell between the effects of thermal conductivity increase due to lack of substrate interactions and the effect of thermal conductivity decrease due to straining. Such dwell and the fact that the bending regions represent a relatively small area of the MXene flake, make the temperature field gradients smoother (figures 4(h)–(m)) than the discontinuities that occur on the non-shocked simply supported flakes condition (figures 5(c), (f), (i), (l) and (o)). The relative size of the unsupported regions in figure 5 is large, compared to the total size of the flake and the bending strained zones of the shocked MXenes over the trenched, circular, radial, and spiral molds in figure 4. By evaluating the temperature gradients between the heat sink and source, but at different regions within the flake (sections 1 and 2 shown in figures 4(b)–(g)), it can be seen that the thermal gradient differences between sections 1 and 2 temperature profiles indicate that different strains through the section's path generate different temperature gradients. Figures 4(h)–(m) shows, through sections 1 and 2 temperature profile differences, that the more geometric discontinuities through a section, the more the thermal gradient variations are established in the temperature profile through that section. However, since strain has less significant effect over the flake's thermal conductivity than the supporting condition (supported/suspended flake), the temperature profiles at

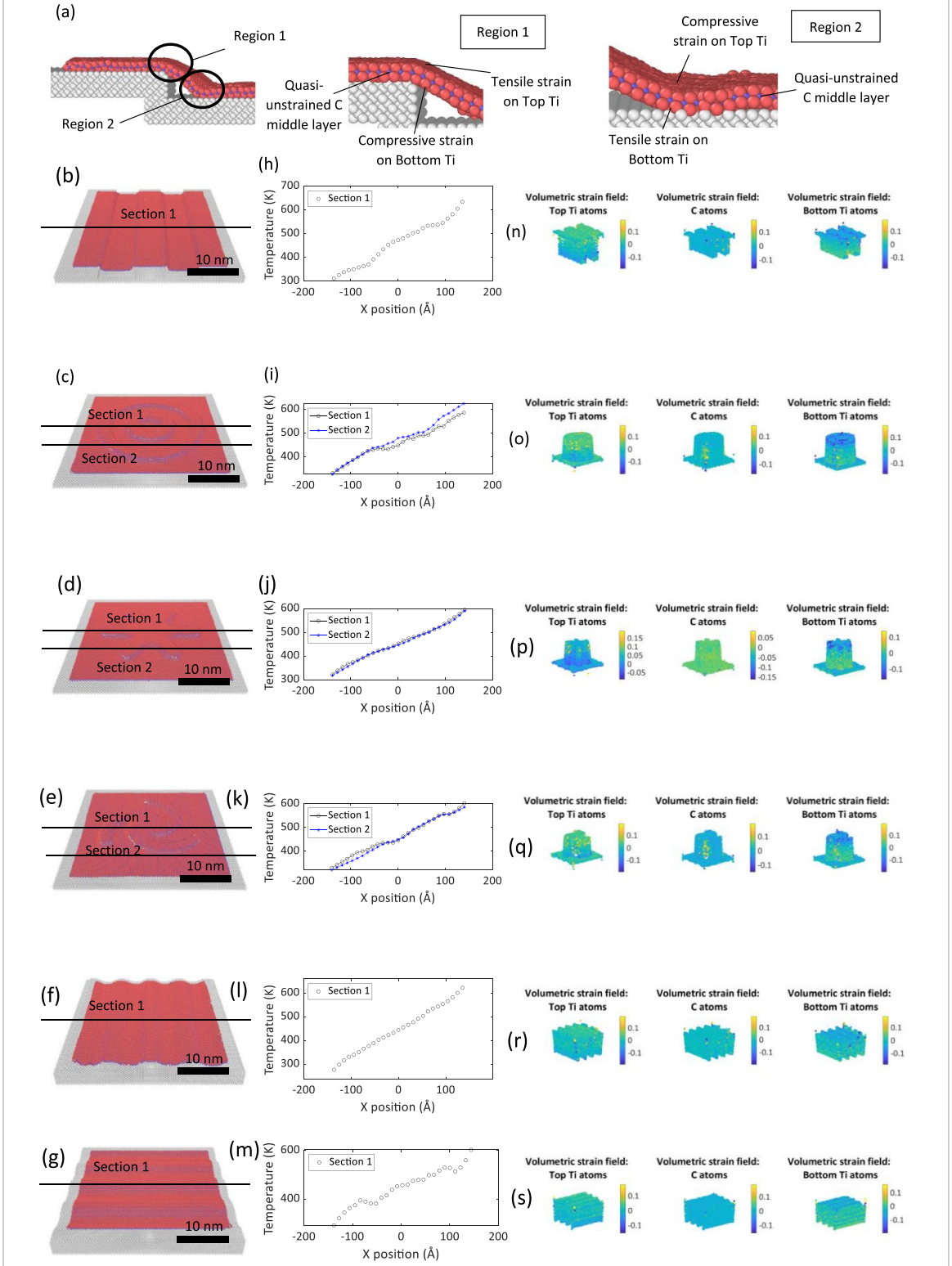

Figure 4. Laser shocked Ti_2C on Si substrates. (a) MD results showing the bent flake geometry, temperature fields, and indicating the compressive and tensile strain regions within the MXene flake. (b)–(g) Substrates shapes. (h)–(m) Temperature fields at the atoms in sections 1 and 2 for the different substrate shapes in the shocked flakes. (n)–(s) Volumetric strain fields in a Ti_2C MXene flake, where the bottom Ti atoms are the ones closer to the Si substrate.

the refions dominated by trenches (section 1) is not significantly off from the temperature profiles at regions far from the substrates' geometric discontinuities (section 2) in figures 4(i)–(k).

Applying shock to a flake to conform it to a substrate is useful if strain can be induced over a significant area of the MXene flake. For that, we simulated shocking a Ti_2C flake over a rounded bump-trenched Si substrate (figures 4(f) and (g)). This substrate geometry maximizes contact with the flake and induces

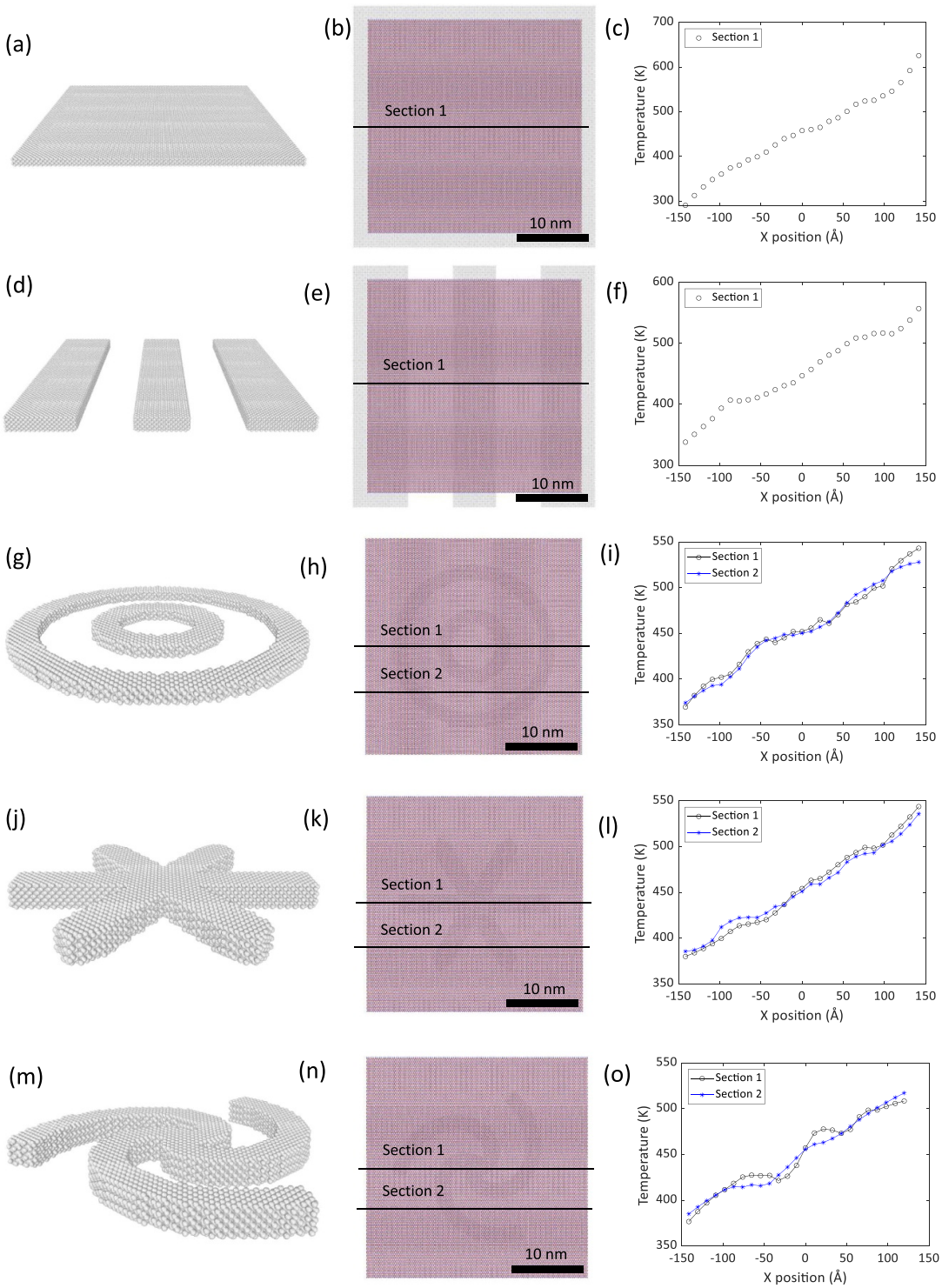

Figure 5. Temperature field dependence on support shapes for simply supported Ti_2C flakes. (a), (d), (g), (j) and (m) Substrates' shapes. (b), (e), (h), (k) and (n) 31.5 nm square Ti_2C single flakes placed over the shaped Si substrates. (c), (f), (i), (l) and (o) Temperature fields at the atoms in sections 1 and 2 for the different substrate shapes at the simply supported flake.

straining through the whole flake, compressing the top Ti atoms, stretching the bottom Ti atoms at the bumps' valleys regions, stretching the top Ti atoms, and compressing the bottom Ti atoms in the bumps' peaks regions. Figure 4(f) shows that the smooth strain variations through the heat flow path generate an equally smooth temperature profile with insignificant temperature gradients variations when compared with sharper geometry changes of the rectangular bumbs in figures 4(b) and (h).

The effect of directionality of the bending strain on the heat flow direction was simulated by rotating the bump directions of 90° (figure 4(g)). Results show that for substrate bumps orientations that generate bending stresses normal to the heat flow, the thermal conductivity is reduced when compared to the flakes

shocked over substrates that generate bending stresses along the heat flow direction, showing that the bending stress directionality affects the phonons scattering, and consequently the thermal conductivity reduction (figures 4(l) and (m)). The last condition (figure 4(m)) has a thermal conductivity similar to the simply supported case, without significant straining in the heat flow in-plane direction.

2.6. Flakes deposition without conformation over shaped substrates for thermal shifting behavior creation

The effect of the Si substrate shape and trenches on the in-plane flake's thermal conductivity, was measured via NEMD simulations of heat transfer in Ti_2C flakes. The heat transfer simulations in a MXene 2D flake deposited on a flat Si substrate (figures 5(a) and (b)) results in a continuous rate of change in temperature between the heat source and sink (figure 5(c)). Simply deposited 2D films on flat substrates are the most straightforward condition to employ in circuit manufacturing since it does not require any special substrate processing. Shaping the Si substrate but depositing the Ti_2C flake without substrate wrapping showed that the temperature field can be altered. The straight-line trenched substrate with deposited MXene 2D flakes (figures 5(d) and (e)) showed that there is a thermal gradient variation in the regions where the flake is suspended (figure 5(f)). Trenching the substrate then is a simple solution to increase the supported flake's overall thermal conductivity in a direction normal to the trenches. The circular-shaped substrate (figures 5(g) and (h)) can be employed to achieve the thermal shield effect, maintaining the temperature variations low in a large portion of the design area (section 1 in figure 5(i)). A smaller temperature change can be seen in regions away from the interactions with the substrate, at the center zone, and the ring zone between the circular Si support regions (section 2 in figure 5(i)). Therefore, if a component or section of the circuit needs to operate at a specific temperature region with low thermal gradients, the circular trenched substrate gives this thermal shield effect. A radial substrate (figures 5(j) and (k)) can be employed to achieve the thermal concentrator effect where a steep temperature gradient is desired within a reduced section (central region of section 1 in figure 5(l)) of the design area while maintaining the remaining regions at low-temperature gradients (section 2 in figure 5(l)). The spiral substrate (figures 5(m) and (n)) can be employed when a thermal inverter effect is desired. The temperature field shows slowing down or even reversing the local temperature gradients (local negative thermal conductivity seen through section 1 in figure 5(o)), compared to the primarily established temperature gradient between the heat sink and source (section 2 in figure 5(o)). All these temperature gradient effects which shape the temperature field are due to the differences between thermal conductivities in regions where the flakes are suspended and regions where they are supported by the substrate.

3. Conclusions

This work paves the way for employing laser shocking as a method for nanoshaping in MXene 2D flakes, which can conform well to substrates with intricate shapes under desired processing conditions. A combination of both substrate and straining conditions (applying laser shocking) allows the production of nanoshaped MXene 2D materials that is interesting for thermal management such as concentrators, inverters, shields, and trenches with alternating high and lower thermal conductivities, providing an interesting methodology for electronic devices design. MD simulations were conducted to understand the effects of substrate and straining conditions on the thermal properties of MXene 2D flakes. After straining, the thermal conductivities of all simulated MXenes considerably drop due to Z phonon modes suppression. Bending strain also showed an effect in the MXenes thermal conductivity drop by scattering phonon modes. This makes MXenes an attractive option for the management of thermal fields. Compared to the strained condition, the larger thermal conductivity changes due to the supporting condition allow us to infer that setting the supporting material and boundary conditions has an effective impact on the design of the metamaterial. A combination of substrate and straining conditions can be applied simultaneously to a design to help tune the flake's thermal conductivity. The applicability of this conclusion based on the simulation results obtained for the Ti_2C single flakes can be extended to the other MXene types since results indicate that the thermal conductivity changes for different supporting and straining conditions for those flakes as well. However, since the thermal conductivity changes for the Ti_2C are more significant for those different conditions, we expect the thermal conductivity engineering using shaped substrates to result in smoother changes when the Ti_3C_2, and $Ti_3C_2O_2$ are employed. This study also reveals the size dependence of thermal conductivity in MXenes as it is highly influenced by the flake size while the thicker MXenes are not too influenced by strains.

4. Methods

4.1. MD simulations

In our MD simulations for the thermal conductivity of the MXenes, the interatomic forces were calculated using the hybrid Lennard Jones and Axilrod Teller potentials [27, 28]. Initially, we parametrized the force field model that consisted of hybrid Lennard-Jones and Axilrod-Teller models (supplementary data (table S1)). This model is valid for flakes without excessive defect density since its parameters were not optimized to consider interatomic interactions at defective flake configurations. Then, we chose to build square titanium carbide flakes with sides measuring 31.5 nm, so the MD environment would be able to replicate the high-frequency (optical) and some low-frequency (acoustic) phonon modes that are crucial for the thermal conductivity determination [22, 29] since such phonon wavelengths are only a few nm for the simulated titanium carbides compositions.

We considered executing the MD simulations for the $Ti_3C_2T_2$, where T could be O, OH, or F, which are terminations that can be present in these flakes. Due to the simplicity of considering the O termination in the determination of the interatomic potential, we chose this termination for our baseline MXene 2D flake so its simulation results could be compared with the thermal conductivity values measured experimentally in other research work [22].

The simulation conditions for the MXene 2D flakes were replicated from the unsupported cases, which only account for in-flake interatomic interactions, to the silicon substrate-supported cases. The only parameters that were included were the potentials to simulate the interactions between the MXenes flakes and the substrate and the Si substrate atoms. As Motlag *et al* [21] showed, the interactions between 2D materials flakes and substrates can be simplified to van der Walls interactions, parametrized only via LJ potentials. In this manner, the optimization process described in the supplementary data (section 1) was repeated to determine the LJ force field parameters for Si–O, Si–C, and Si–Ti interactions (supplementary data (table S1)). In the MD simulations, we fixed the atomic coordinates of the silicon substrate atoms, by setting the forces acting over them as 0 on the 3 axes, while the substrate interaction forces were kept on the MXene 2D flakes. Therefore, the simulation would not lose Si atoms due to the laser shocking conditions.

For the laser shocking NEMD simulations to obtain the strained thermal conductivities as a function of trenches aspect ratios (depth/width), the flakes were accelerated over the trenched substrate and its energy was equivalent to the experimental laser shock energy density. In these NEMD simulations, different trenches aspect ratios were employed, by keeping the trench width constant and varying the trench's depth.

The MD simulations were executed in LAMMPS [24], and the visualization of results was done in OVITO [30]. In the NEMD simulations, the flakes had the atoms located in their extremities, at the zig-zag direction, on the *X*-axis, constrained for displacements in this direction, and the atomic forces were set as zero for these atoms. The system's temperature was set as 400 K and the first simulation stage was intended for the system to achieve thermal equilibrium, employing an *NVT* (constant number of atoms *N*, constant volume *V*, and constant temperature *T*) ensemble. Then, the atoms at one of the extremities were set to move at a constant velocity for a predefined time interval, while the atoms at the other extremity remained fixed. Another interval was run for the strained system to achieve equilibrium at the new strained state. Then, an *NVE* (constant number of atoms *N*, constant volume *V*, and constant system's energy *E*) ensemble was set. A heat source and a heat sink were created in these groups, to generate a temperature gradient that was checked when equilibrium was achieved, after 600 000-time steps for flake lengths smaller than 650 nm and 2400 000 time steps for flake lengths larger than 650 nm, with step durations of 1 fs for the size dependence NEMD simulations.

For the strained MXenes MD simulations, 315 Å $\times$ 315 Å MXene 2D flakes were fixed at one end and a constant displacement rate was applied to the atoms on a small strip region at the opposite end, through the *x*-axis. A heat source, able to produce 2 eV ps^{-1}, and a heat sink, able to remove 2 eV ps^{-1}, were set at the opposite ends of the flake, through the zig-zag direction, where the heat sink was located between -150 Å and -135 Å and the heat source was located at 135 Å and 150 Å. An NVE ensemble was set, and the temperature varied between the heat sink and source. This simulation was repeated for different strains, at suspended condition, supported over flat Si mold condition, and shocked over a single trench Si mold with different aspect ratios (width/depth).

The special substrates for the metamaterial design (nanopillars, trenches, circular, radial, spiral, and bumps) MD simulations were executed with the same configuration as the strained simulations with Ti_2C simply supported at the substrates and shocked over them. The shock pressure was simulated by applying an atomic force of 0.2 eV $Å^{-1}$ for 10 ps. A shock simulation video can be seen in the supplementary data.

4.2. DFT calculations

The DFT calculations for the force field model parametrizations were executed with QE [23]. We have employed ultrasoft pseudopotentials with Pedrew–Burke–Ernzerhof functional, 25 Ry for energy cutoff, 225 Ry for charge cutoff, and a $3 \times 3 \times 1$ grid of K-points for the self-consistent field calculations to determine the system's energy of a unit cell of the simulated MXenes (Ti_2C, Ti_3C_2, and $Ti_3C_2O_2$).

4.3. Thermal conductivity calculation

The phonon-based thermal conductivity of the MXenes can be determined using the Klemens theory:

$$k_p = \frac{\rho}{T}\sum_j \frac{\langle \vartheta_j \rangle^4}{\langle \gamma_j^2 \rangle}\frac{1}{\omega_{\max,j}}\ln\left(\frac{\omega_{\max,j}}{\omega_{\min,j}}\right) \tag{2}$$

where ρ is the flake's density, T is the simulation temperature, $\langle \vartheta_j \rangle$ is the average group velocity, γ_j is the average value of the Grüneisen parameter for the jth branch, $\omega_{\min,j}$ and $\omega_{\max,j}$ are the minimum and maximum circular frequencies of the jth branch, and the size (L) dependent term is $\omega_{\min,j}$, which can be determined via:

$$\omega_{\min,j} = \left(\frac{M\omega_{\max,j}\langle \vartheta_j^3 \rangle}{2k_B TL\langle \gamma_j^2 \rangle}\right)^{\frac{1}{2}} \tag{3}$$

where M is the mass within a unit cell, k_B is the Boltzmann constant, and L is the flake length. Therefore, the higher the flake length, the higher the thermal conductivity.

Equations (2) and (3) when combined, indicate a logarithmic relationship between k_p and L, represented by equation (1).

We investigated the influence of strain on the thermal conductivity of titanium carbides via NEMD simulations to check if strain and thermal conductivity are correlated for the MXenes. The established temperature gradient, associated with the magnitude of heat input on the source and sink, and with the flake's dimensions, was used to determine the thermal conductivity (k_p) of the simulated flake via:

$$k_p = \frac{qL}{A\Delta T} \tag{4}$$

where q is the magnitude of the heat source and sink input to the system, L is the flake length, A is the flake's cross-section area, and ΔT is the temperature difference between the flake's extremities, through the length.

4.4. Strain calculations

Figures 3(d), (f) and (h) schematically shows the simulation loads and boundary conditions. As the system reached the mechanical equilibrium, a heat source and a heat sink were applied close to the edges where the external load and the mechanical constraints were set. Then, the flake's mean strain on the x-axis was determined through:

$$\varepsilon_x = \frac{\Delta l_x}{L_{0x}}. \tag{5}$$

The volumetric atomic strain is obtained by:

$$\varepsilon_V = E_{XX} + E_{YY} + E_{ZZ} \tag{6}$$

where E is the atomic Green–Lagrangian strain tensor:

$$E = \frac{1}{2}\left(F^T F - I\right) \tag{7}$$

where F is the deformation gradient tensor.

Data availability statement

All data that support the findings of this study are included within the article (and any supplementary files).

Acknowledgment

The authors thank the support from Office of Research, Purdue University. This research was partially supported by the National Science Foundation through NSF-ExpandQISE award #2228841.

ORCID iDs

Danilo de Camargo Branco https://orcid.org/0000-0003-2637-6359
Gary J Cheng https://orcid.org/0000-0002-1184-2946

References

[1] Naguib M, Kurtoglu M, Presser V, Lu J, Niu J, Heon M, Hultman L, Gogotsi Y and Barsoum M W 2011 Two-dimensional nanocrystals produced by exfoliation of Ti_3AlC_2 *Adv. Mater.* **23** 4248–53
[2] Gogotsi Y and Anasori B 2019 The rise of MXenes *ACS Nano* **13** 8491–4
[3] Naguib M, Mashtalir O, Carle J, Presser V, Lu J, Hultman L, Gogotsi Y and Barsoum M W 2012 Two-dimensional transition metal carbides *ACS Nano* **6** 1322–31
[4] Anasori B, Lukatskaya M R and Gogotsi Y 2017 2D metal carbides and nitrides (MXenes) for energy storage *Nat. Rev. Mater.* **2** 1–17
[5] Naguib M, Mochalin V N, Barsoum M W and Gogotsi Y 2014 25th anniversary article: MXenes: a new family of two-dimensional materials *Adv. Mater.* **26** 992–1005
[6] Qin R, Shan G, Hu M and Huang W 2021 Two-dimensional transition metal carbides and/or nitrides (MXenes) and their applications in sensors *Mater. Today Phys.* **21** 100527
[7] Kurtoglu M, Naguib M, Gogotsi Y and Barsoum M W 2012 First principles study of two-dimensional early transition metal carbides *MRS Commun.* **2** 133–7
[8] Borysiuk V N, Mochalin V N and Gogotsi Y 2018 Bending rigidity of two-dimensional titanium carbide (MXene) nanoribbons: a molecular dynamics study *Comput. Mater. Sci.* **143** 418–24
[9] Lipatov A, Lu H, Alhabeb M, Anasori B, Gruverman A, Gogotsi Y and Sinitskii A 2018 Elastic properties of 2D $Ti_3C_2T_x$ MXene monolayers and bilayers *Sci. Adv.* **4** 1–8
[10] Plummer G, Anasori B, Gogotsi Y and Tucker G J 2019 Nanoindentation of monolayer $Ti_{n+1}C_nT_x$ MXenes via atomistic simulations: the role of composition and defects on strength *Comput. Mater. Sci.* **157** 168–74
[11] Maleski K, Ren C E, Zhao M Q, Anasori B and Gogotsi Y 2018 Size-dependent physical and electrochemical properties of two-dimensional MXene flakes *ACS Appl. Mater. Interfaces* **10** 24491–8
[12] Mathis T S, Maleski K, Goad A, Sarycheva A, Anayee M, Foucher A C, Hantanasirisakul K, Shuck C E, Stach E A and Gogotsi Y 2021 Modified MAX phase synthesis for environmentally stable and highly conductive Ti_3C_2 MXene *ACS Nano* **15** 6420–9
[13] Li J, Qin R, Yan L, Chi Z, Yu Z, Li N, Hu M, Chen H and Shan G 2019 Plasmonic light illumination creates a channel to achieve fast degradation of $Ti_3C_2T_x$ nanosheets *Inorg. Chem.* **58** 7285–94
[14] Li J, Chi Z, Qin R, Yan L, Lin X, Hu M, Shan G, Chen H and Weng Y X 2020 Hydrogen bond interaction promotes flash energy transport at MXene-solvent interface *J. Phys. Chem.* C **124** 10306–14
[15] Song H, Liu J, Liu B, Wu J, Cheng H M and Kang F 2018 Two-dimensional materials for thermal management applications *Joule* **2** 442–63
[16] Li X, Maute K, Dunn M L and Yang R 2010 Strain effects on the thermal conductivity of nanostructures *Phys. Rev.* B **81** 245318
[17] Zhang C, Hao X L, Wang C X, Wei N and Rabczuk T 2017 Thermal conductivity of graphene nanoribbons under shear deformation: a molecular dynamics simulation *Sci. Rep.* **7** 1–8
[18] Hong Y, Li L, Zeng X C and Zhang J 2015 Tuning thermal contact conductance at graphene-copper interface via surface nanoengineering *Nanoscale* **7** 6286–94
[19] Gholivand H, Fuladi S, Hemmat Z, Salehi-Khojin A and Khalili-Araghi F 2019 Effect of surface termination on the lattice thermal conductivity of monolayer $Ti_3C_2T_z$ MXenes *J. Appl. Phys.* **126** 065101
[20] Park G, Kang S, Lee H and Choi W 2017 Tunable multifunctional thermal metamaterials: manipulation of local heat flux via assembly of unit-cell thermal shifters *Sci. Rep.* **7** 1–15
[21] Motlag M, Hu Y, Tong L, Huang X, Ye L and Cheng G J 2019 Laser-shock-induced nanoscale kink-bands in WSe_2 2D crystals *ACS Nano* **13** 10587–95
[22] Zha X H, Huang Q, He J, He H, Zhai J, Francisco J S and Du S 2016 The thermal and electrical properties of the promising semiconductor MXene Hf_2CO_2 *Sci. Rep.* **6** 1–10
[23] Giannozzi P *et al* 2009 QUANTUM ESPRESSO: a modular and open-source software project for quantum simulations of materials *J. Phys.: Condens. Matter* **21** 395502
[24] Plimpton S 1995 Fast parallel algorithms for short-range molecular dynamics *J. Comput. Phys.* **117** 1–19
[25] Postmus C, Ferraro J R and Mitra S S 1968 Pressure dependence of infrared eigenfrequencies of KCl and KBr *Phys. Rev.* **174** 983–7
[26] Saavedra H M, Mullen T J, Zhang P, Dewey D C, Claridge S A and Weiss P S 2010 Hybrid strategies in nanolithography *Rep. Prog. Phys.* **73** 036501
[27] de Branco D C and Cheng G J 2021 Employing hybrid Lennard-Jones and Axilrod-Teller potentials to parametrize force fields for the simulation of materials' properties *Materials* **14** 6352
[28] Borysiuk V N, Mochalin V N and Gogotsi Y 2015 Molecular dynamic study of the mechanical properties of two-dimensional titanium carbides $Ti_{n+1}C_n$ (MXenes) *Nanotechnology* **26** 1–10
[29] Klemens P G 1981 Theory of lattice thermal conductivity: role of low-frequency phonons *Int. J. Thermophys.* **2** 55–62
[30] Stukowski A 2010 Visualization and analysis of atomistic simulation data with OVITO-the Open Visualization Tool *Model. Simul. Mater. Sci. Eng.* **18** 015012